FEBS Letters 352 (1994) 247–250

FEBS 14578

Real-time analysis of the calcium-dependent interaction between calmodulin and a synthetic oligopeptide of calcineurin by a surface plasmon resonance biosensor

Emiko Takano, Masakazu Hatanaka, Masatoshi Maki*

Laboratory of Human Tumor Viruses, Institute for Virus Research, Kyoto University, 53 Shogoin-Kawahara-cho, Sakyo-ku, Kyoto 606-01, Japan

Received 3 August 1994

Abstract The calcium-dependent interaction between calmodulin (CaM) and the synthetic oligopeptide of a predicted CaM-binding region of human calcineurin A-2 was analysed with an automated surface plasmon resonance biosensor, BIAcore. The oligopeptide was immobilized to a biosensor chip via the amino-terminal cysteine residue by a thiol–disulphide exchange method. The biosensor chip was regenerated by an EGTA-containing buffer after each analysis. Kinetics experiments showed that CaM bound with a high affinity to the oligopeptide in a Ca^{2+}-dependent manner. The estimated rate constants of association (k_{ass}) and dissociation (k_{diss}) were 2.3×10^5 $M^{-1} \cdot s^{-1}$ and 3.9×10^{-3} s^{-1}, respectively. The ratio of k_{diss}/k_{ass}, 1.7×10^{-8} M, was in good agreement with the dissociation constant (K_d) of 2.4×10^{-8} M determined from the equilibrium phase.

Key words: Calmodulin; Calcineurin; Calcium-dependent; Surface plasmon resonance; Biosensor

1. Introduction

Calmodulin (CaM) is a ubiquitous Ca^{2+}-binding protein involved in a variety of Ca^{2+}-dependent signaling pathways in eukaryotic cells, and regulates the activities of a large number of proteins including protein kinases, phosphatases, and calcium pumps as well as those involved in motility [1,2]. CaM with 148 residues containing four helix-loop-helix (EF-hand) Ca^{2+}-binding structures is known to recognize a short segment of 20–30 residues in the target proteins [3,4]. There is no obvious sequence homology among the CaM-binding regions, but they have propensity to form basic amphiphilic α-helical structures [3]. Recently, some three-dimensional structures of complexes between CaM and CaM-binding oligopeptides have been elucidated [5–7]. Binding affinities between CaM and these target oligopeptides have been analysed by several methods including competition assays using myosin light chain kinase, circular dichroism specroscopy, electrophoretic mobility shift assay and fluorometric methods [8]. The fluorometric methods involve either measuring changes of intrinsic tryptophan fluorescence of the peptides upon binding to CaM which contains no tryptophan residue [9] or measuring the fluorescence change of dansylated CaM with unlabeled peptides [10]. Rate constants of association and dissociation, however, could not be easily determined by these conventional methods.

The recently developed BIAcore biosensor instrument allows real-time analyses of biospecific interactions by detecting surface plasmon resonance (SPR) signals, and is applicable to various studies on structure–function relationships of macromolecules of interest [11]. Employing the BIAcore system, we demonstrate for the first time the Ca^{2+}-dependent interaction between CaM and the synthetic oligopeptide of the previously predicted CaM-binding region in calcineurin, a Ca^{2+}/CaM-dependent protein phosphatase [12,13].

*Corresponding author. Fax: (81) (75) 751-3998.

Abbreviations: EDC, *N*-ethyl-*N'*-(dimethylaminopropyl)carbodiimide; NHS, *N*-hydroxysuccinimide; CaM, calmodulin; SPR, surface plasmon resonance; PDEA, 2-(2-pyridinyldithio)ethaneamine hydrochloride.

2. Material and methods

2.1. Materials

A 25-residue oligopeptide containing the predicted CaM-binding region in human calcineurin A-2 [13,14] with a cysteine residue added at its N-terminus, designated as CNApep25, was custom-synthesized by Sawaday Technology Inc. (Tokyo, Japan). CaM purified from bovine brain was obtained from Sigma Chemical Co. (St. Louis, USA). A sensor chip CM5, a coupling reagent kit and a 10% solution of Tween 20 (Surfactant P20) were from Pharmacia Biosensor AB (Uppsala, Sweden). The other reagent grade chemicals were purchased from Nacalai Tesque (Kyoto, Japan) or Wako Pure Chemicals (Osaka, Japan).

2.2. Surface plasmon resonance measurements

Real-time analysis of Ca^{2+}-dependent interaction between CaM and the calcineurin oligopeptide was performed with a BIAcore instrument (Pharmacia Biosensor AB). The principle and application of the system employing the method of surface plasmon resonance (SPR) detection was described by Karlsson et al. [11]. Coupling of oligopeptide CNApep25 to the sensor chip CM5 was performed by the ligand thiol method as described [15]. A continuous flow of HBS buffer (10 mM HEPES, pH 7.4, 0.15 M NaCl, 3.4 mM EDTA, 0.005% Tween 20) passing over the sensor surface was maintained at 5 μl/min. The carboxylated dextran matrix was activated by injection of 10 μl of a solution containing 0.2 M EDC and 0.05 M NHS, and modified by injection of 20 μl of 80 mM PDEA in 0.1 M borate buffer, pH 8.5. Next, 35 μl of 50 μg/ml CNApep25 solution in 50 mM formate, pH 4.0, was injected and the oligopeptide was immobilized via thiol–disulphide exchange reaction. Finally, a 20 μl of 50 mM cysteine–1 M NaCl was injected to deactivate excess reactive groups and to wash out unbound oligopeptides.

The SPR measurements for the binding of CaM to the immobilized CNApep25 were performed at 2 μl/ml in Buffer F (20 mM Tris-HCl, pH 7.5, 150 mM NaCl, 1 mM EGTA, 1.5 mM $CaCl_2$, 0.005% Tween 20). The sensor chip was regenerated after each analysis cycle by injecting 6 μl of Buffer F without $CaCl_2$, and then initialized with continuous flow of Buffer F.

3. Results and discussion

Calcineurin, a Ca^{2+}/CaM-dependent serine/threonine-specific protein phosphatase, is a heterodimer of a 61 kDa catalytic subunit (calcineurin A) and a 19 kDa regulatory subunit (calcineurin B) [12]. This phosphatase is now known to be inhibited by immunophillins, the binding proteins of immunosuppressive

SSDI 0014-5793(94)00965-1

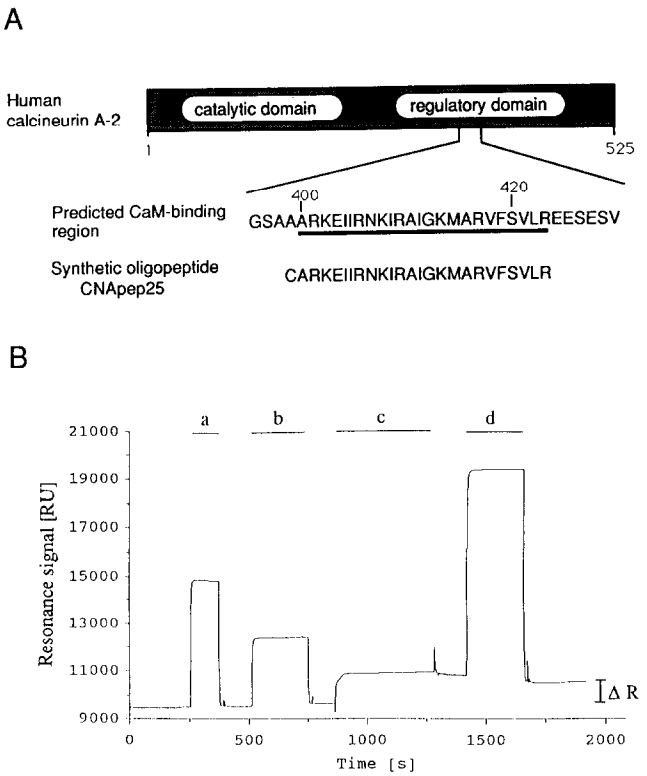

Fig. 1. Immobilization of the synthetic oligopeptide of calcineurin A. (A) A sequence of the 25-residue oligopeptide used in the present study. The oligopeptide, designated as CNApep25, corresponds to the predicted CaM-binding region in human calcineurin A-2 and contains an added cysteine at the N-terminus. (B) A sensorgram of immobilization of oligopeptide CNApep25 by the thiol ligand method. The bars indicated by a, b, c and d refer to the stages in the immobilization procedure: a, activation of sensor chip by NHS/EDC; b, modification by PDEA; c, immobilization of ligand (CNApep25); d, deactivation and washing with 50 mM cysteine–1 M NaCl. ΔR indicates the amount of immobilized ligand (880 RU).

drugs cyclosporin A and FK506 [16]. CaM binds to calcineurin A, and its potential binding site was predicted by Kincaid et al. [13] by comparing the sequence with those of the known CaM-binding regions in other proteins, but direct binding of CaM to such a sequence in calcineurin A has not been reported. Fig. 1A shows the amino acid sequence of a potential CaM-binding synthetic oligopeptide CNApep25, corresponding to residues 400–423 of human calcineurin A-2 [14] with an additional cysteine residue at the N-terminus. The oligopeptide was immobilized to a BIAcore sensor chip using a thiol coupling reagent PDEA as shown in Fig. 1B. Since 1000 RU is equivalent to a change in surface concentration of about 1 ng/mm^2 for most macromolecules [15], the amount of the immobilized ligand was estimated to be 880 pg/mm^2 from the increased resonance signal (ΔR) of 880 RU.

CaM solutions of various concentration were passed over the CNApep25-immobilized biosensor chip in the presence of Ca^{2+}, where the amounts of bound CaM were detected as changes of SPR signals, and expressed as relative response. Fig. 2A displays an example of overlaid sensorgrams using five different concentrations of CaM (12.5–500 nM). The rates of association and values of relative response at equilibrium depended on the concentrations of CaM as shown in the association phase (arrow a). Washing the sensor chip with the running buffer caused gradual decrease of the SPR signals, indicating a time-dependent dissociation of CaM from the immobilized CNApep25 (dissociation phase, arrow b). The sensor chip was easily stripped of bound CaM by the buffer without Ca^{2+} as indicated by the drop of the SPR signal to the base line level (regeneration phase, arrow c).

Rates of association (dR/dt) using various concentrations of CaM were analysed with kinetics evaluation software installed in the BIAcore. The plots of dR/dt vs. relative response gave linear relationships (Fig. 3A). The negative values of the slopes (apparent association rate constant, k_{app}, at each concentration of CaM) were re-plotted against CaM concentration (Fig. 3B). The association rate constant (k_{ass}) was obtained from the slope: $k_{ass} = 2.3 \times 10^5\ M^{-1} \cdot s^{-1}$. The plot of steady state binding levels (R_{eq}, relative response at equilibrium) vs. CaM concentrations gave a saturation curve, indicating a specific interaction of CaM with DNApep25 (Fig. 4). The dissociation constant (K_d) determined by Scatchard plot (inset) was 2.4×10^{-8} M. R_{max} (maximum binding capacity) was calculated to be 1800 RU, or 1800 pg/mm^2.

Assuming a one-to-one stoichiometric interaction between CaM and CNApep25, the oligopeptide accessible to CaM was calculated to be about 37% based on their molecular weights and observed response (immobilized oligopeptide: 0.3 pmol/mm^2, CNApep25, M_r = 2929; maximum CaM-binding: 0.11 pmol/mm^2, CaM, M_r = 16,680). Thus, CaM could not bind to about 63% of the immobilized CNApep25 molecules which might have been buried far inside the dextran matrix or positioned too close one another to be accessible to the large molecule.

For the dissociation phase analysis, the effect of re-binding of released CaM to the immobilized CNApep25 was examined. At the end of association, 2 μM CNApep25 solution was injected to compete for CaM-binding with the immobilized oligopeptide. As shown in Fig. 5A, this procedure accelerated an apparent dissociation rate, suggesting a considerable contribution of re-binding . Thus, the dissociation rate constant was

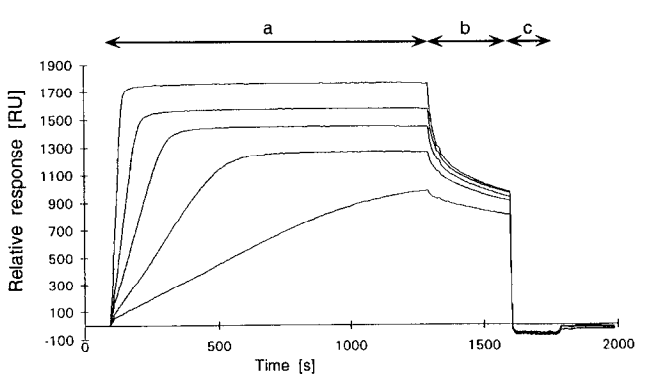

Fig. 2. Representative overlaid sensorgrams illustrating the real-time binding of CaM at various concentrations (25, 50, 100, 200 and 500 nM, from bottom to top) to the oligopeptide CNApep25 immobilized on the biosensor chip. Analysis was performed with Buffer F (20 mM Tris-HCl, pH 7.5, 150 mM NaCl, 1 mM EGTA, 1.5 mM $CaCl_2$, 0.005% Tween 20). Arrows indicate phases of (a) association, (b) dissociation and (c) regeneration. Regeneration was performed by washing the sensor chip with Buffer F without Ca^{2+}.

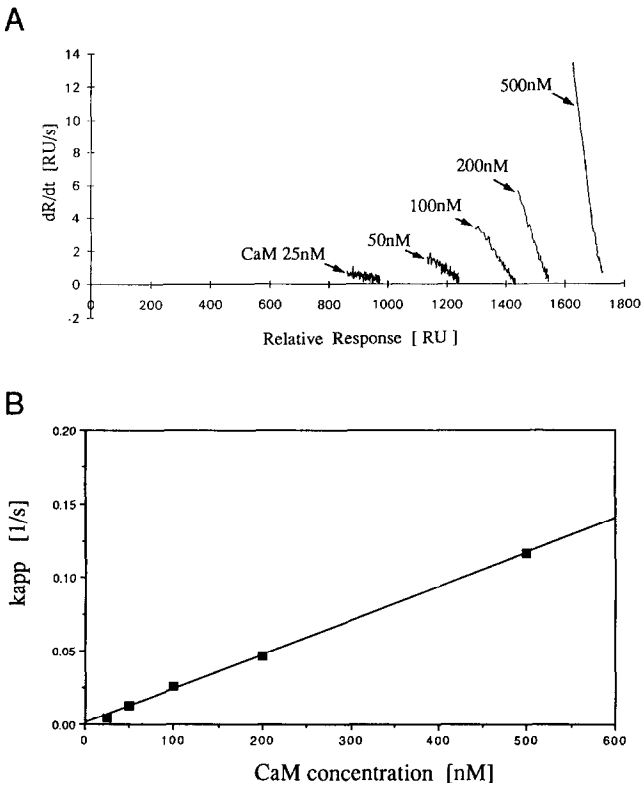

Fig. 3. Determination of the association rate constant. A, plots of association rates (dR/dt) vs. relative response by analysis of the association phase in Fig. 2. Apparent first-order rate constants (k_{app}) were obtained from the slopes according to equation $dR/dt = k_{ass}CR_{max} - k_{app}R$, where R, binding value expressed as relative response; C, concentration of sample; t, time; k_{ass}, association rate constant. (B) A plot of k_{app} vs. CaM concentration. The slope gave a value of k_{ass} from the equation $k_{app} = k_{ass}C + k_{diss}$, where k_{diss} is a dissociation rate constant. $k_{ass} = 2.3 \times 10^5\ M^{-1} \cdot s^{-1}$.

determined by analysis of the dissociation phase in the presence of free CNApep25. The first-order reaction plot revealed two components with different dissociation rates (Fig. 5B). The calculated dissociation rate constant (k_{diss}) of the major slower component (59.7%, designated R_s) and the minor faster component (40.3%, designated R_f) was $3.9 \times 10^{-3}\ s^{-1}$ and $2.1 \times 10^{-2}\ s^{-1}$, respectively. There is a possibility, however, that the acceleration of the apparent dissociation rate of the complex by addition of free CNApep25 was caused by interaction of the oligopeptide with the pre-formed complex at any second binding site in CaM, and not by blocking the re-binding of liberated CaM to the immobilized CNApep25. The analysis of dissociation phase in the absence of CNApep25 gave a k_{diss} value smaller than $10^{-3}\ s^{-1}$; an accurate constant could not be obtained due to the significant residual binding (Fig. 5A, – CNApep25).

The ratio of the obtained dissociation rate constant (k_{diss}(slow) = $3.9 \times 10^{-3}\ s^{-1}$, Fig. 5B) and the association rate constant ($k_{ass} = 2.3 \times 10^5\ M^{-1} \cdot s^{-1}$, Fig. 3B) was calculated to be 1.7×10^{-8} M. This value was in good agreement with the dissociation constant (K_d) of 2.4×10^{-8} M determined from the equilibrium phase by Scatchard plot analysis (Fig. 4). There are several possible reasons for the presence of the fast and slow dissociating components (Fig. 5B). First, the conformation of the immobilized oligopeptide may be heterogeneous depending on the site of the matrix of the sensor chip. The oligopeptide CNApep25 is very basic (calculated isoelectric point, pI = 12.35) and the structure should be significantly affected electrostatically by the surrounding acidic charges of the carboxylated dextran matrix. Second, isomerization may occur in the complex between CaM and CNApep25 from an intermediate form (fast dissociation) to a tight form (slow dissociation) during the association phase. Third, some of CaM molecules used in the present study may be partly denatured, and the defective protein may have a lower affinity. Considering the effect of re-binding in kinetics evaluation, further studies are required to pursue the cause of the biphasic nature of the dissociation .

Using ^{125}I-labeled CaM, Hubbard and Klee [17] reported kinetics of CaM-binding to purified calcineurin which was immobilized on nitrocellulose membrane filters. The reported dissociation constant (K_d) determined by equilibrium binding analyses was 1.6×10^{-8} M, which agrees with our data ($K_d = 2.4 \times 10^{-8}$ M, Fig. 4). Rate constants, however, were 20–40 times different (in the present study: $k_{ass} = 2.3 \times 10^5\ M^{-1} \cdot s^{-1}$, k_{diss}(slow) = $3.9 \times 10^{-3}\ s^{-1}$; reported: $k_{ass} = 8.9 \times 10^3 M^{-1} \cdot s^{-1}$, $k_{diss} = 8.5 \times 10^{-5}\ s^{-1}$). Although the basis of discrepancy is not clear, the greater association rate as revealed in the present study meets better the physiological demand that CaM binds to the target protein more rapidly in response to an increase of intracellular Ca^{2+} ($t_{1/2}$ at 100 nM CaM: 30 s in this study; 13 min in their study) .

Kinetic analyses by the automated SPR biosensor system are fast and simple, and the system should be useful to analyse interactions between CaM or other Ca^{2+}-binding proteins and their target proteins with high molecular weight since the biosensor chip is easily regenerated under a mild condition with a Ca^{2+}-chelating reagent.

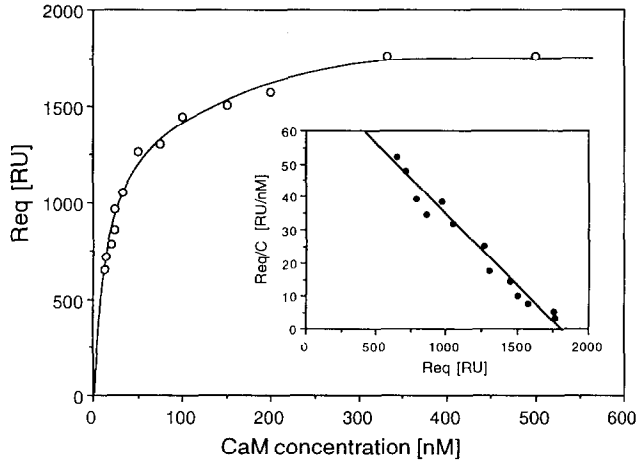

Fig. 4. Scatchard plot analysis for determination of the dissociation constant. CaM concentrations ranged from 12.5 nM to 500 nM, and data similar to those for Fig. 2 were recorded. Longer injection times were used for concentrations below 50 nM to ensure that steady state (equilibrium) was reached. Relative response expressed as steady state binding values (R_{eq}) and CaM concentrations are plotted as indicated (○). (Inset) Scatchard plot. The reciprocal of the slope gave a value of the dissociation constant (K_d) of 2.4×10^{-8} M from the following equation: $R_{eq}/C = R_{max}/K_d - R_{eq}/K_d$. R_{eq}, steady state binding value; C, CaM concentration; R_{max}, maximum binding capacity of the immobilized peptide.

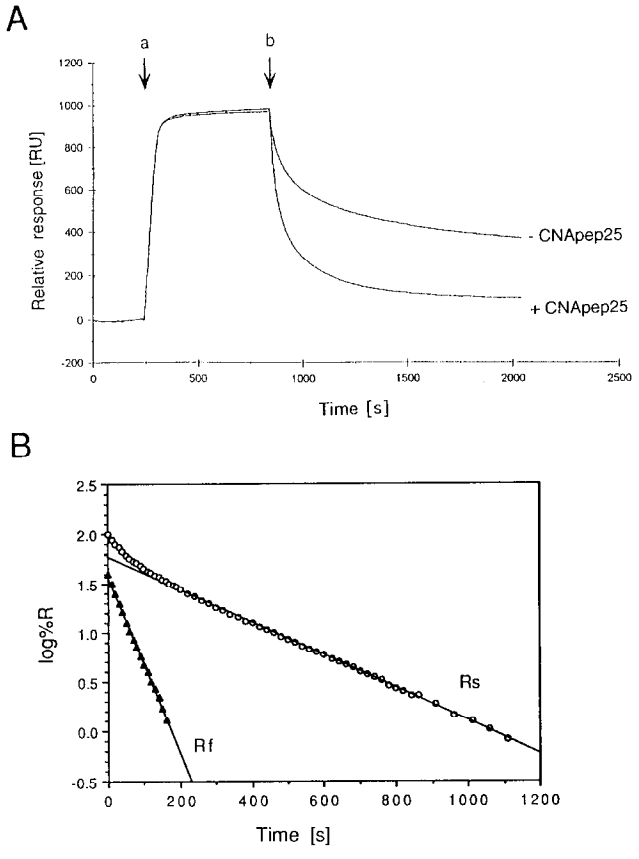

Fig. 5. Determination of dissociation rate constant. (A) Sensorgrams illustrating dissociaton of CaM from the immobilized CNApep25. Association start point is indicated by arrow a. At the end of association, indicated by arrow b, a 30 μl solution of either Buffer F (−CNApep25) or 2 μM CNApep25 in Buffer F (+CNApep25) was injected. (B) First-order reaction plot of dissociation in the presence of the oligopeptide. A value of 90 RU was subtracted as base-line response (undissociable component and effect of the CNApep25 solution on SPR response). The dissociation rate constant (k_{diss}) for the slower dissociation component (R_s) was obtained from the slope of the linear line fitting well to the plots (○) in the later phase. The relative amount of the fast dissociation component (R_f) in the earlier dissociation phase was calculated by subtracting the theoretical amount of slower dissociation component (R_s) from the observed response (○), and was re-plotted in the semi-logarithmic scale (▲). The calculated rate constants are: k_{diss}(slow) = 3.9×10^{-3} s^{-1}; k_{diss}(fast) = 2.1×10^{-2} s^{-1}.

Acknowledgements: We are indebted to Professor K. Nagata of the Institute for Chest Disease for the BIAcore system. We also thank Professor T.E. Martin of the University of Chicago for reading this manuscript.

References

[1] Klee, C.B. and Vanaman, T.C. (1982) Adv. Protein Chem. 35, 213–321.
[2] Kakiuchi, S. and Sobue, K. (1983) Trends Biochem. Sci. 8, 59–62.
[3] O'Neil, K.T. and DeGrado, W.F. (1990) Trends Biochem. Sci. 15, 59–64.
[4] McPhalen, C.A., Strynadka, N.C.J. and James, M.N.G. (1991) Adv. Protein Chem. 42, 77–144.
[5] Ikura, M., Clore, G.M., Gronenborn, A.M., Zhu, G., Klee, C.B. and Bax, A. (1992) Science 256, 632–638.
[6] Meador, W.E., Means, A.R. and Quiocho, F.A. (1992) Science 257,1251–1255.
[7] Meador, W.E., Means, A.R. and Quiocho, F.A. (1993) Science 262,1718–1721.
[8] Erickson-Vitanen, S. and DeGrado, W.F. (1987) Methods Enzymol. 139,455–478.
[9] Buschmeier, B., Meyer, H.E. and Mayr, G.W. (1987) J. Biol. Chem. 262,9454–9462.
[10] Vorherr, T., James, P., Krebs, J., Enyedi, A., McCormick, D.J., Penniston, J.T. and Carafoli, E. (1990) Biochemistry 29, 355–365.
[11] Karlsson, R., Michaelsson, A. and Mattsson, L. (1991) J. Immunol. Methods 145, 229–240.
[12] Klee, C.B., Draetta, G.F. and Hubbard, M.J. (1988) Adv. Enzymol. 61, 149–200.
[13] Kincaid, R.L., Nightingale, M.S. and Martin, B.M. (1988) Proc. Natl. Acad. Sci. USA 85, 8983–8997.
[14] Guerini, D. and Klee, C.B. (1989) Proc. Natl. Acad. Sci. USA 86,9183–9187.
[15] BIAcore Methods Manual, Pharmacia Biosensor AB.
[16] Liu, J., Farmer, J., Lane, W., Friedman, J., Weissman, I. and Schreiber, S. (1991) Cell 66, 807–815.
[17] Hubbard, M.J. and Klee, C.B. (1987) J. Biol. Chem. 262, 15062–15070.